Environmental Toxicology and Pharmacology 53 (2017) 64–73

Contents lists available at ScienceDirect

Environmental Toxicology and Pharmacology

journal homepage: www.elsevier.com/locate/etap

Research paper

The protective study about alleviation of simvastatin on the damages of PEG-BNs in mice

Wenzhen An[a], Biao Han[b], Kang Li[a], Shahnaz Akhtar[a], Ying Zhang[a], Xuan Zhang[a], Xueli Sha[a], Lan Gao[a,*]

[a] School of Life Sciences, Lanzhou University, Lanzhou, Gansu 730000, China
[b] The First Hospital of Lanzhou University, Thoracic surgery, Lanzhou, Gansu 730000, China

ARTICLE INFO

Keywords:
PEG-BNs
Damages
Simvastatin
Anti-inflammatory
Mice

ABSTRACT

Boron nitride nanoparticles have been proved to cause various toxicities, damages or inflammations after entering into *in vivo* in previous reports. However, up to now, there are rare investigations about the alleviation of damages caused by nanoparticles *in vivo* through natural small molecule drugs. Therefore, in this work, PEG-BNs with high solubility was successfully synthesized, and then their biodistribution in mice were studied using radiolabeling technique. And the heart, lung, liver, spleen, kidney tissues and blood samples were done for histology and biochemical analysis. The results showed that PEG-BNs were mainly distributed in lung, liver, kidney and spleen with an obviouse decreasing distribution as the experimental time was increasing. Besides, significantly serum biochemical and tissue pathological changes induced by PEG-BNs were confirmed. Moreover, after simvastatin (SST) exposure to the PEG-BNs model mice, the damages and biochemical indexes were recovered significantly as compared to the single exposure group mice in serum, which indicates a good treatment effect on the toxicity of PEG-BNs *in vivo* in mice. This study provides some basic data and useful information for the treatment of damages caused by the nanoparticles in mice in the future.

1. Introduction

Boron nitride (BN), known as white graphene, are structurally analogues with graphene in which C atoms are replaced by the alternating B and N atoms (Chhowalla et al., 2013; Elkady et al., 2012; Joshi et al., 2014; Raccichini et al., 2015; Wang et al., 2012; Xu et al., 2013). Based on the structural characteristics, BN demonstrate improved lubricating properties, resistance to chemical attack and oxidation, high thermal conductivity, excellent temperature stability, low thermal expansion, better heat conductivity and excellent electrical insulation (Lin et al., 2009; Mosleh et al., 2009; Wu et al., 2001). Therefore, for special chemical and physical characteristics of BN nanoparticles, many researchers have used these nanoparticles in biomedical domain, such as the drug carriers, nano-imaging and nanotransducers (Danti et al., 2014; Weng et al., 2014; Zhang et al., 2013). However, before the clinical application of these nanoparticles, it is very important to investigate the biosafety both *in vivo* and *in vitro* (Ciofani et al., 2010; Liu et al., 2015; Weber et al., 1993). Many nanoparticles taken *via* oral or intravenous injection into the body are mainly distributed in liver, kidney and lung so as to lead to various inflammations in these organs. These nanoparticles include carbon nanoparticles, gold nanoparticles, silver nanoparticles and other metal and mental-oxide nanoparticles (Batista et al., 2017; Ciofani et al., 2014; Qi et al., 2014; Seiffert et al., 2015; Sendra et al., 2017). Compared to the carbon and other metal nanoparticles, BN nanoparticles have not been explored extensively in their damages or toxicity for body, up to now, only few works have been reported on investigating the toxicity and biosafety of BN nanoparticles *in vivo*.

It is well known that damage is the chief toxicity concern surrounding nanotechnology, and excessive exposure to nanoparticles with high concentration requires urgent elimination of the accumulated nanoparticles from biological organs as well as the treatment of inflammatory disorders. Therefore, some researchers have tried to study several anti-inflammatory drugs on the treatment of toxicity of nanoparticles *in vivo*, and they found that those anti-inflammatory drugs could promote the excretion of nanoparticles that are accumulated in the body to certain extent in order to reduce or eliminate the tissue inflammatory (Carvalho et al., 2012; Shah et al., 2011; Tu et al., 2013). Clinically, statins were mainly used for anti-inflammatory, cardiovascular and cerebrovascular diseases (Carvalho et al., 2012; Endres, 2006; Rezende et al., 2015; Shah et al., 2011). Researchers have also praised stains for their ability to reduce cancer risks (Khurana

* Corresponding author.
E-mail address: gaolan@lzu.edu.cn (L. Gao).

http://dx.doi.org/10.1016/j.etap.2017.04.021
Received 20 January 2017; Received in revised form 28 April 2017; Accepted 29 April 2017
Available online 01 May 2017
1382-6689/

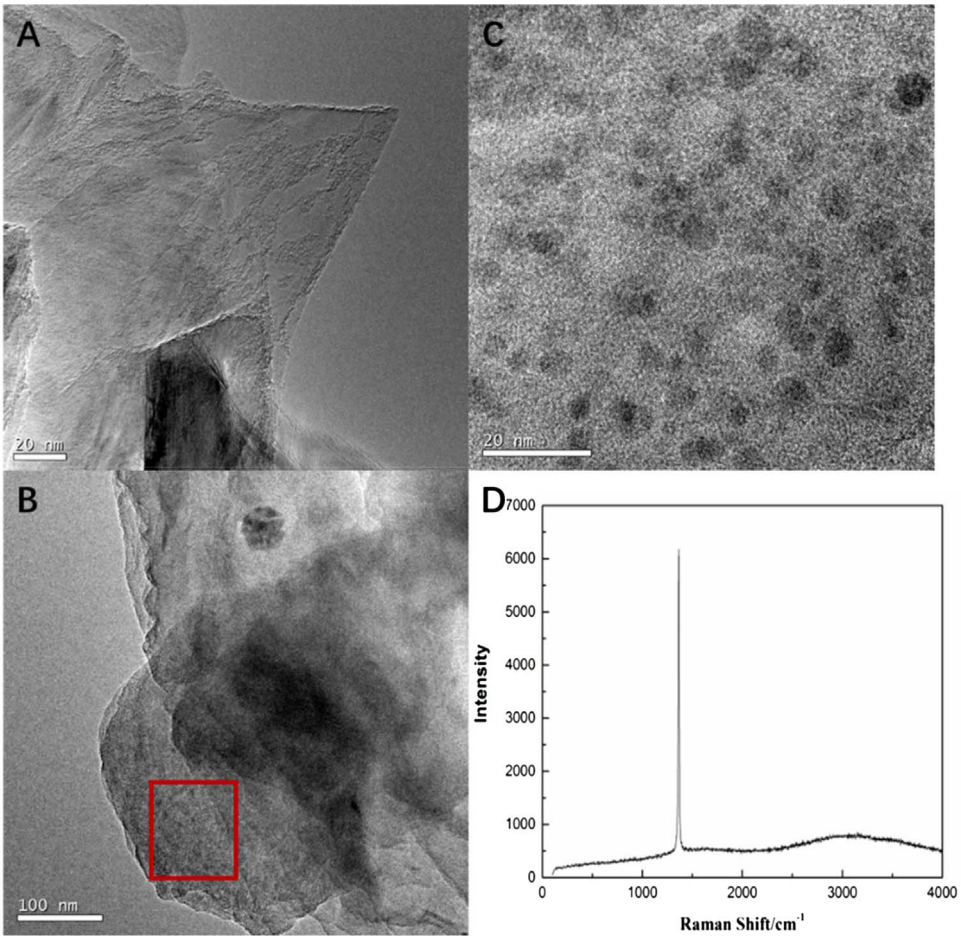

Fig. 1. TEM and Raman spectra of PEG-BNs.

et al., 2007; Simon et al., 2014; Wang et al., 2013; Yang et al., 2015). In addition, recent studies have shown that the stains can improve the bioavailability of the nanoparticles by promoting their excretion from the body (Ganesh et al., 2015; Raju, 2014). Simvastatin, one of nine known stains (atorvastatin, cerivastatin, fluvastatin, lovastatin, mevastatin, pitavastatin, pravastatin, rosuvastatin, and simvastatin), is well known for its effects on cellular proliferation and inflammation and is widely used for preventing cardiovascular events and cancer (Kochuparambil et al., 2011). However, as far as we know, rare investigation has been performed to study the protective effect of simvastatin on mice model of tissue damage caused by the BN nanoparticles.

Considering that poor solubility and biocompatibility of BN materials make it too difficult to be used in biomedical applications, in this work, the PEG coated BN (PEG-BNs) were prepared successfully as reported in the previous literatures (Weng et al., 2014) to improve the water solubility and reduce the toxicity level of pristine BN, then we investigate the tissue distribution of PEG-BNs based on ^{131}I-labeled in mice *in vivo*. Additionally, the prevention and treatment capabilities of simvastatins (SST) on the toxicity of PEG-BNs in mice were explored. To the best of our knowledge, this is the first detail study of this kind to investigate the treatment of toxicity of BN nanoparticles *in vivo*.

2. Materials and methods

2.1. Synthesis and characterization of PEG-BNs

Solution of 6-arm-polyethyleneglycol-amine (Sunbio Inc.) (3 mg/mL) was mixed with BN sheets (0.5 mg/mL) (purchased from Baoding Zhong Pu Rui Tuo Technology. LTD), and the mixture was stirred at 200 °C for 4 d under the steady nitrogen flow environment. After cooling the reaction mixture to room temperature, about 60 mL H_2O was added for the extraction purpose (Shah et al., 2011). The solution was sonicated and centrifuged at 4000 rpm for 20 min, and the supernatants were collected and dialyzed for about 1 week by dialysis membrane (MD25) to remove the free PEG. Finally, the solution was dried at 50 °C in a vacuum oven, and the solid product in the form of PEG-BN was obtained. The prepared samples were then characterized by TEM (Tecnai G2 F30), XRD (XRD 600), Raman spectroscopy and thermogravimetric analysis and so on.

2.2. ^{131}I labeling PEG-BN and yield measurement

Na^{131}I (about 1.5 mCi) was provided by The First Hospital of Lanzhou University. According to the literature (Wang et al., 2004; Yang et al., 2011), chloramine-T method was used to label PEG-BNs with Na^{131}I. The labelled mixtures were centrifuged at 12,000 rpm for 10 min to purify ^{131}I PEG-BNs, and the supernatant was discarded to remove the free Na^{131}I. The yields of the labelled compounds were measured with paper chromatogram under the chromatographic solutions of normal saline and acetone. If the labelling yield was obtained over 60%, then the labelled compounds could effectively reflect their real distribution and metabolism *in vivo*.

2.3. Tissue distribution study

Kunming mice (female, about 15–18 g) were provided by the Laboratory Centre for Medical Science, Lanzhou University, Gansu, China. All animals were housed in individual cages with controlled environment at 21–22 °C and the lights were kept on from 08:00 to

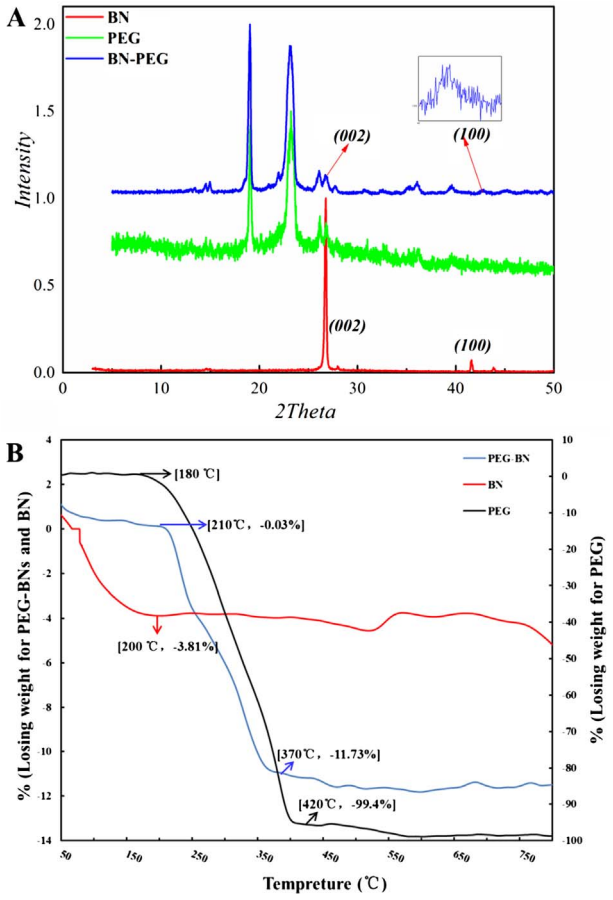

Fig. 2. XRD and TGA characterizations of BN, PEG and PEG-BNs.

20:00 h. The mice were fed ad libitum with food and tap water. The animals were kept under the human care according to the Principles of the Laboratory Animal Care Formulated by the National Society of Medical Research and guide for the US National Institutes of Health. ^{131}I PEG-BNs solutions (200 μg/mouse) were injected intravenously to different groups of mice (5 mice/group). The animals were sacrificed at 1, 6, 16 and 24 h post injection; heart, lung, liver, spleen and kidney tissues were immediately dissected. About 1–2 mL of blood was collected from each mouse. Each tissue was wrapped in foil and weighed, and then the radioactivity of ^{131}I was measured. In the next step, the pharmacokinetic and biodistribution of PEG-BNs were obtained using the following equation:

$$\text{organ uptake} = \frac{\text{organ radioactivity}}{\text{total radioactivity} \times \text{organ weight(g)}} \times 100\%$$

2.4. Dosage effect on the toxicity of PEG-BN in mice

In this experiment, 20 mice were divided into 4 groups. Three groups were intravenously injected with PEG-BN at different dose of 150 μg/mouse, 300 μg/mouse and 450 μg/mouse (0.2 mL), and the forth group was treated with normal saline of 0.9% as the control group. All of the mice were sacrificed after 24 h and their blood was collected and stored for about 2 h at room temperature. Then the serum was obtained through centrifugation and stored in −20 °C refrigerator for use.

2.5. Effects of SST on the toxicity of PEG-BN in mice

Three processes were carried out to investigate the effects of SST on the damages of PEG-BNs in mice, namely, preventive effect, treatment effect and synergistic effect. For the preventive effect experiment, three group's mice were injected with SST using 0 μg/mouse, 150 μg/mouse, 300 μg/mouse and 450 μg/mouse (0.2 mL) respectively on the first and second days. And then all of the mice were exposed with 300 μg/mouse PEG-BNs on the third day, and sacrificed to obtain serum at the fourth day; For the treatment effect experiment, the PEG-BNs model mice were developed through injecting all the mice with 300 μg/mouse PEG-BNs (0.2 mL) on the first day. Then the model mice were grouped and injected intravenously with SST of 0 μg/mouse, 150 μg/mouse, 300 μg/mouse and 450 μg/mouse on the second and third days, respectively, and then all of the mice were sacrificed to obtain serum at the fourth day; For the synergistic effect experiment, the mice were intravenously injected with PEG-BNs and SST [(300 μg PEG-BNs + 0 μg SST)/mouse, (300 μg PEG-BNs + 150 μg SST)/mouse, (300 μg PEG-BNs + 300 μg SST)/mouse and (300 μg PEG-BNs + 450 μg SST)/mouse] simultaneously on the first day, and then all the mice were deal with at the second day. One group of normal mice were dealt with the same process to obtain serum as the control group.

The concentrations of blood urea nitrogen (BUN), creatinine (CREA), cystatin C (Cys-C), alanine aminotransferase (ALT), aspartate aminotransferase (AST) and total bilirubin (TB) in the serum were measured using ELISA Kit. Mice from each group were dissected, and their heart, liver, spleen, lung and kidney tissues were collected. These tissues were stored in 10% buffered formalin and processed for the routine histology with hematoxylin and eosin staining. The tissues were then microscopically observed using microscopy imaging system (Axio Scope.A1, Oberkochen, Germany).

2.6. Statistical analysis

Each data point was reported as the mean value (± sem) of the multiple data points. Statistical significance in the difference was calculated by analysis of variance (ANOVA), and all these statistical calculations were carried out using *SPSS* software.

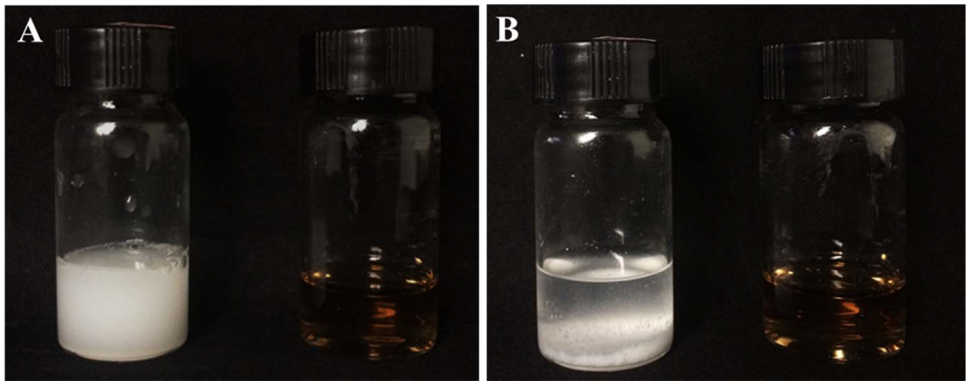

Fig. 3. The water soluble of BN and PEG-BNs after 1 min and 24 h standing. A is in 1 min, B is in 24 h the white is origin BN and the brown is PEG-BNs.

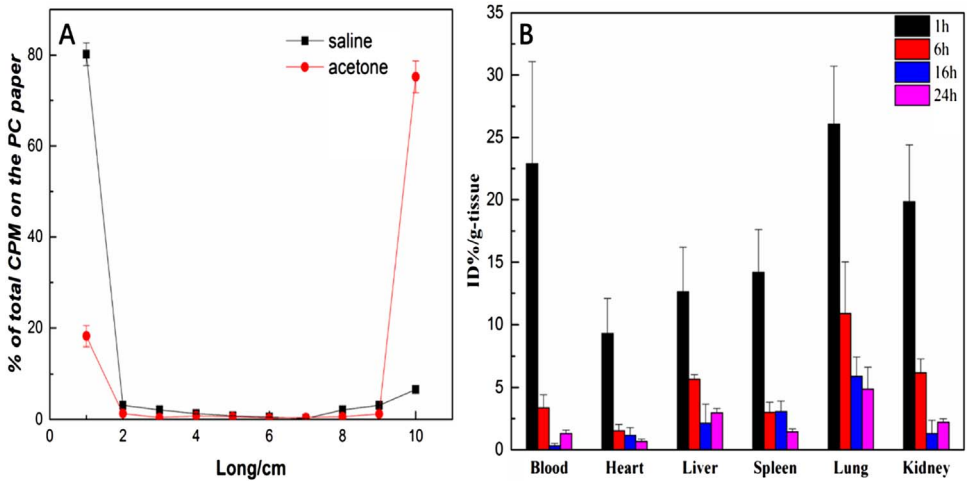

Fig. 4. The radiolabeling yields of ^{131}I PEG-BNs in saline and acetone (A), and the biodistribution of PEG-BNs in blood, heart, liver, spleen, lung and kidney in 24 h after exposure to mice (+sem).

3. Results and discussion

3.1. Preparation and characterization of PEG-BNs

Fig. 1 displays the TEM images of the raw BN and PEG-BNS, which shows that the morphology of the raw BN is highly disordered with a thick layer structure of 2D. After coating with PEG, the size and shape of PEG-BNS became relatively uniform and smooth with clear stripe structure of 2D. This may be resulted of that the raw BN were exfoliated and the bigger size of BN were removed during the preparation process. In addition, the structure of BN was not changed after being coated with PEG (Fig. 1). Fig. 1D shows the Raman spectrum, which confirms the successful preparation of BN coated with PEG. The XRD results of PEG-BNs are shown in Fig. 2A, and it is seen that the peak intensity of PEG is much larger than the BN in the coated samples, this represents that the degree of PEG coating is sufficiently high, thus we have observed high water solubility in the solution containing PEG-BN as shown in Fig. 3, the PEG-BN show good water solubility during 24 h, but the origin BN solution displays some precipitations after 24 h. TGA results of PEG-BNs are showed in Fig. 2B. Because of its good thermal stability, the weight of boron nitride has small variations with temperature increase; however, the thermal stability of PEG is poor, so the thermal stability line of PEG-BNs shows that the residues represent the BN nanoparticles that was ~11.73% in PEG while the PEG-BNs were ~88.27%.

3.2. Tissue biodistribution

Pristine BN are insoluble in water, however, it can be easily dissolved in water after coating with PEG due to its hydrophilic nature. In order to track the PEG-BNs *in vivo*, we have labeled PEG-BN with ^{131}I by adapting a strategy similar to the ^{131}I-labeling of carbon nanotubes (Wang et al., 2004). Briefly, the ^{131}I were introduced by chloramines-T oxidization of $^{131}I^-$ that were likely conjugated to the edges which can detect BN where dangling bonds exist (Yang et al., 2011). The radiolabeling stability of ^{131}I PEG-BNs was tested using 0.9% sodium chloride and acetone by paper chromatogram as shown in Fig. 4, and the radiolabeling yields were found to be 80.2% for saline measurements and 75.2% for acetone measurements, respectively. Both of them were observed to be over 60%, and so the radiotracing technique used in this work reflects the actual biodistribution and behavior of ^{131}I-compounds effectively *in vivo*.

Fig. 4 shows that PEG-BNs that are mainly distributed in the liver, spleen and lung in 24 h, however, their distribution is relatively lower in other tissues, This is in accordance with biodistribution of other carbon nanoparticles (Qi et al., 2014; Wei et al., 2012). As previous articles have reported that the distribution in liver and lung is the highest for graphene oxide, carbon nanotubes and nano-diamonds (Li et al., 2011). Therefore, the results of PEG-BNs distribution here shows a good agreement with graphene oxide coated by PEG (Yang et al., 2011). It is well known that nanoparticles are foreign matter for the living organism. When the nanoparticles enter into the living organism, the tissues with bound reticuloendothelial systems such as liver and spleen would largely uptake those foreigner nanoparticles. Since these organs are macrophage organs with a lot of Kupffer cells, which could devour the nanoparticles to decrease the tissues toxicity. However, as compared to other nanoparticles, the high accumulation of PEG-BNs in the lung was due to the capture role of the pulmonary capillary bed on nanoparticles (Qi et al., 2014). But after being coated with PEG, the biocompatibility of BN was improved up to the great extent and in addition, the size of PEG-BNs was smaller than that of the raw BN nanoparticles. So the PEG-BNs could cross the pulmonary capillary bed and enter into the other tissues with the blood circulation, and most of them are devoured by the Kupffer cells which are finally secreted out from the body through kidneys.

In Fig. 4 the maximum biodistribution of PEG-BNs can be seen at about 1 h post injections. The kidney is the excretory system, so the nanoparticles could be excreted through urine and causes high distribution in kidney. In this work, the accumulation of PEG-BNs in tissues was decreased with the passage of time, while high biodistribution in kidney was observed during the experimental time, this shows that the PEG-BNs could be excreted with time through the urination process. However, there is also an accumulation of PEG-BNs in tissues after 24 h post injection *in vivo*, and this long retention of PEG-BNs in tissue might damage to mice.

3.3. Dosage effect of PEG-BNs on toxicity in mice

In order to study the damage effects of different dosage of PEG-BN to the mice *in vivo*, partial typical biochemical indexes including BUN, CREA, Cys-C, ALT, AST and TB in serum were measured (Fig. 5). It is seen that all of the content show a significant difference in serum of 300 μg/mouse PEG-BN injection group mice compared with the control group mice ($*p < 0.05$), and the contents of ALT, AST and BUN show a significant difference in serum of 450 μg PEG-BNs injection group mice compared with that of the control group mice ($*p < 0.05$). It is noticeable that only the content of Cys-C shows a significant difference in serum of 150 μg PEG-BNs injection group mice compared with that of the control group mice ($*p < 0.05$). This shows that the dosage of 300 μg/mouse can damage effectively tissues of mice *in vivo*, which is the reason why we selected the dosage of 300 μg/mouse as the PEG-BNs

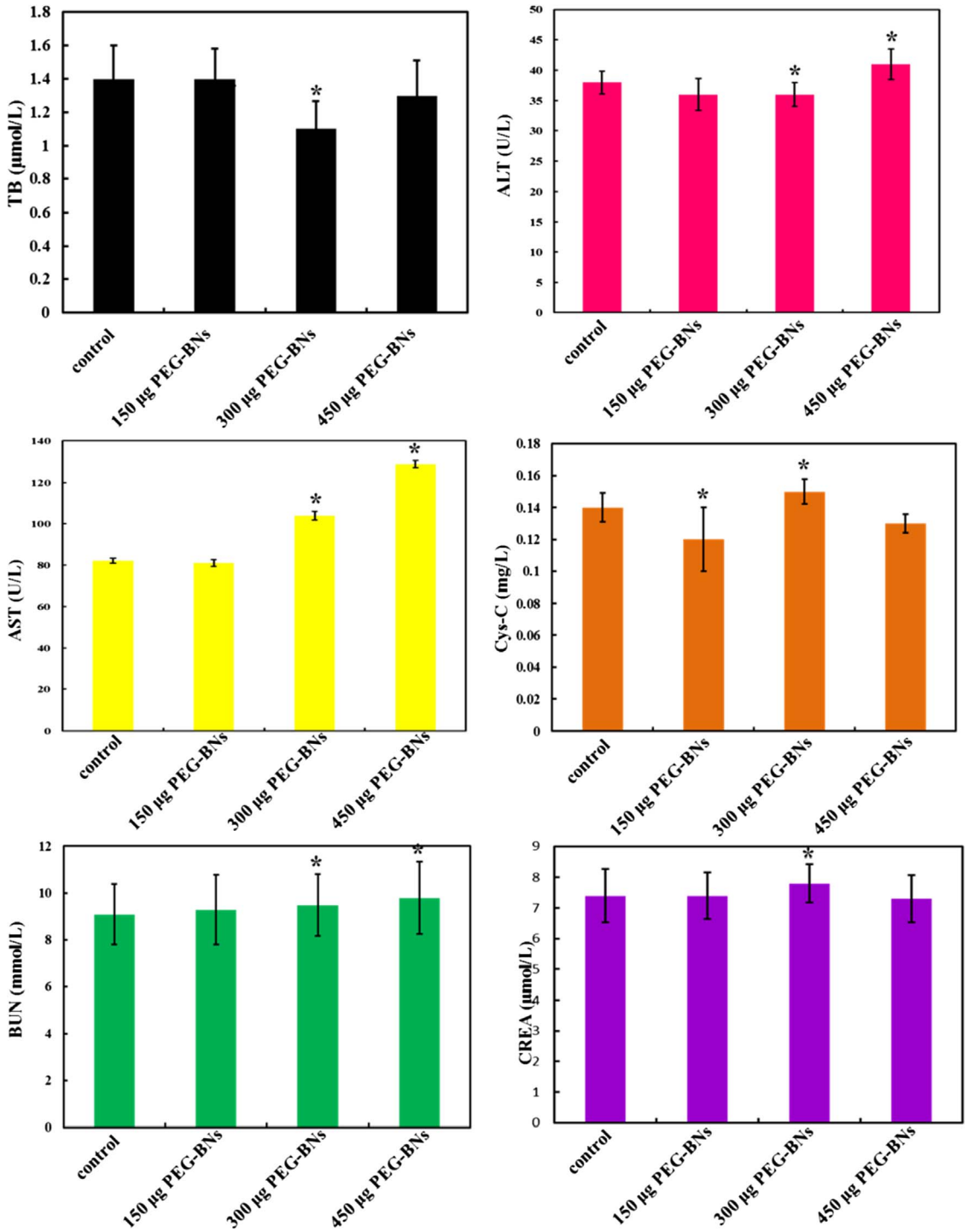

Fig. 5. Biochemical indexes content in serum after PEG-BNs exposure to mice (*$p < 0.05$ for the different concentration group *vs.* control group. ± sem).

model concentration in the following experiment.

3.4. Effect of SST on toxicity of PEG-BNs in mice

SST was used to give relief to the damage effect of PEG-BNs in this work. Moreover, in order to investigate the effect of SST on toxicity of PEG-BNs, the biochemical indexes and tissues histology of mice were measured, these biochemical indexes include BUN, CREA, Cys-C, ALT, AST and TB in serum of prevention/treatment and synergistic group mice.

The prevention effect of SST on the damage of PEG-BNs in mice is shown in Fig. 6. In the figure it can be seen that almost all investigations of biochemical indexes have the significant difference compared with the control group and single PEG-BNs exposure group (*$p < 0.05$, $^{\&}p < 0.05$). This indicates that SST shows negative prevention effect on the damage of PEG-BNs to the mice, and the prevention effect of SST has no dosage-dependence in mice.

The treatment effect of SST on the damage of PEG-BNs in mice can be seen in Fig. 7. At the dosage of 150 μg/mouse SST, the indexes of ALT and Cys-C show no significant differences compared with the control group while the others show a significant difference (*$p < 0.05$), all these indexes show a significant difference compared with the single PEG-BNs exposure group ($^{\&}p < 0.05$). At the dosage of 300 μg/mouse SST, the levels of Cys-C and CREA recover to the normal

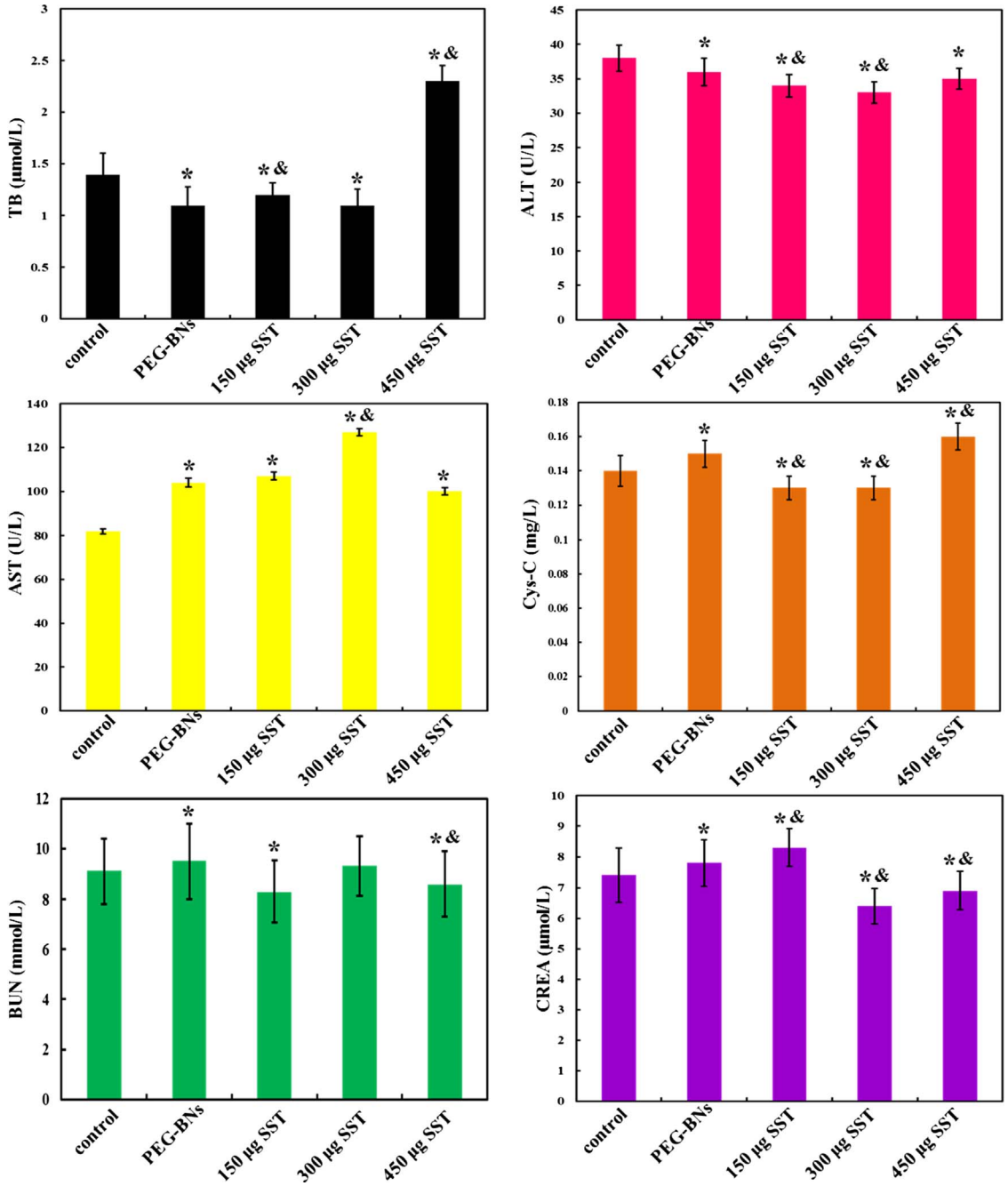

Fig. 6. Biochemical indexes content in serum in SST prevention group mice (*$p < 0.05$ for the different concentration group *vs.* control group; &$p < 0.05$ for the prevention group *vs.* single PEG-BNs group. ± sem).

level. Compared with the single PEG-BNs exposure group, almost all of the indexes show significant differences except that of ALT (&$p < 0.05$). At the dosage of 450 μg/mouse SST, only BUN show no significant difference compared with the control group and the single PEG-BNs exposure group, while the others show a significant difference (*$p < 0.05$, &$p < 0.05$). These results indicate that SST shows partially positive treatment effect on the damage of PEG-BNs in mice and the dosage of 300 μg/mouse shows a better treatment effect. However, it is observed that this treatment effect has no dosage-independency within the dosage scope of the work. This means that appropriate dosage SST can be used to treat the damage of PEG-BNs nanoparticles.

For the synergistic group shown in (Fig. 8), SST shows a positive effect on the damage of PEG-BNs. Compared with the control group, CREA can recover to the normal level at the dosage of 150 μg/mouse SST, and AST, Cys-C,TB, and CREA can recover to the normal level at the dosage of 300 μg/mouse and 450 μg/mouse SST (*$p < 0.05$). Compared with the single PEG-BNs exposure group, the AST, TB, Cys-C and CREA don't show a significant difference (&$p < 0.05$). All these results indicate that SST shows a positive synergistic effect on the damage of PEG-BNs, which might be result out that the biocompatibility of PEG-BNs is further improved by SST.

Based on the above analysis, SST has a positive treatment and synergistic effect but these effects are not dosage-independent, which may own to that stains can increase the level of ALT and AST rather than increasing the risk of liver damage (De Keyser et al., 2014; Simon et al., 2014), and to a certain degree, excess stains can lead to chronic glomerulonephritis (Abaci et al., 2015; Cheungpasitporn et al., 2015; Hou et al., 2013; Yang et al., 2015). From these results, we can see that the dosage of 300 μg/mouse SST provides better effect to the toxicity of

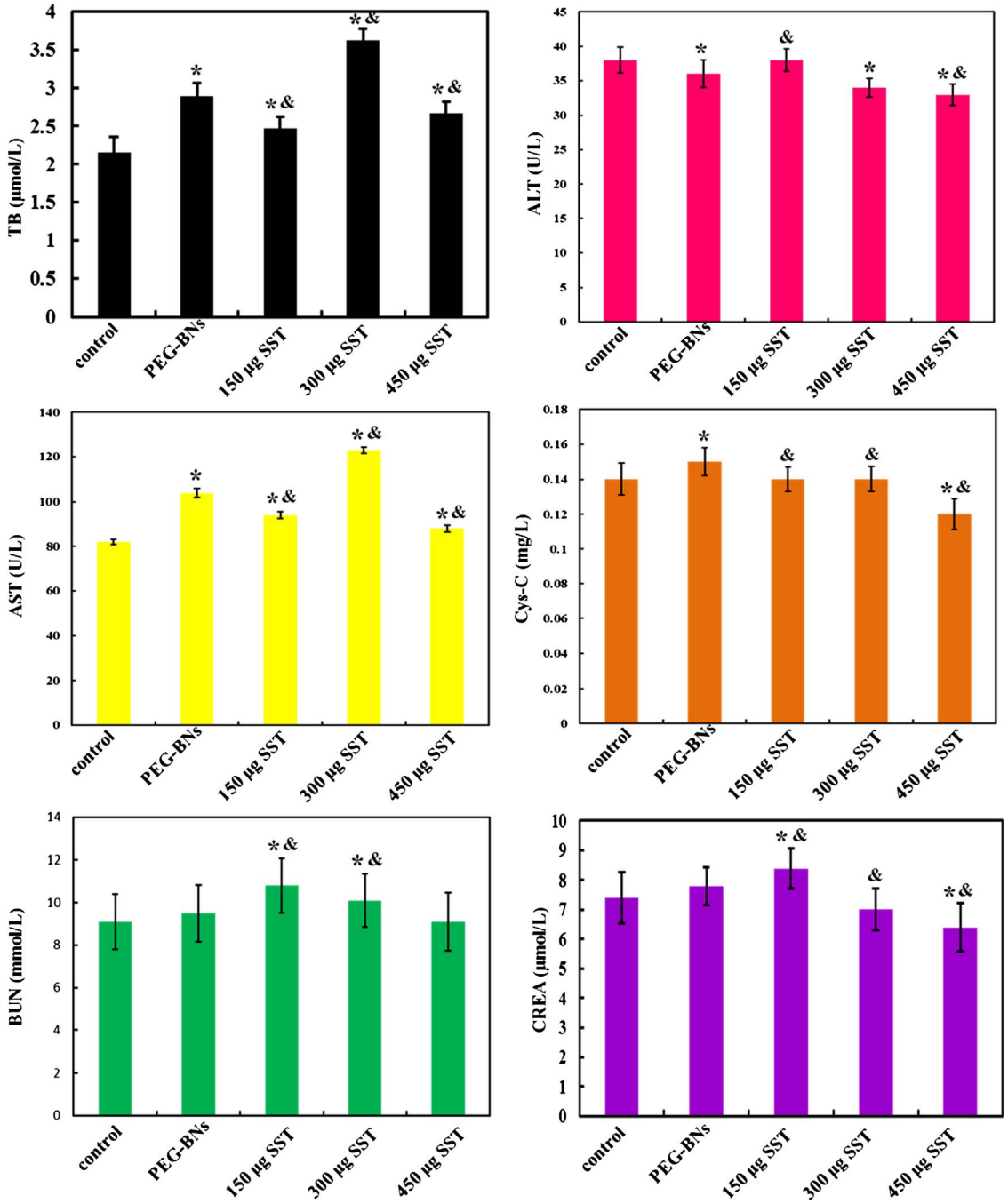

Fig. 7. Biochemical indexes content in serum in SST treatment group mice (*$p < 0.05$ for different concentration group *vs.* control group; $^{\&}p < 0.05$ for the prevention group *vs.* single PEG-BNs group. ± sem).

PEG-BNs in mice. This shows that SST can be expected to be a good medicine to relieve the damage of PEG-BNs to the body *in vivo*.

3.5. Tissue histology study

According to these results, we choose dosage of 300 μg/mouse SST and 300 μg/mouse PEG-BNs to inject to the mice and to further evaluate the effect of PEG-BNs and SST; the tissues histology was measured after injecting PEG-BNs or SST in mice. In this work, the exposure concentration of 300 μg/mouse PEG-BNs was selected for its obvious damage effect to mice through previous dosage-dependence investigation. The results showed that the PEG-BNs could cause extensive damages on tissues of liver, spleen, kidney, lung and heart compared to that of the control group (Fig. 9). After exposure to PEG-BNs, disorder in hepatic cord and bleeding in hydropic degeneration can be seen, moreover, edema and some cell membrane are disrupted in splenic tissue, and small vessels in the spleen can also be seen there. Alveolar wall thickening, epithelial cell rupture, bronchial epithelial disorder and serve to bleed could also be observed in lung tissues. Besides, the severe lesion was observed from pathological section of the heart and kidney tissue (Fig. 9). Hence, the PEG-BNs could cause serious damages on the tissues of mice *in vivo*. Compared with previous reports on the toxicity of nanoparticles that was mainly on lung, liver, spleen and kidney (Wei et al., 2012), the heart showed an obvious damage after PEG-BNs injection in this work which is in according with results of Abdelhalim M.A.K et al. reported (Abdelhalim and Jarrar, 2011). They reported that the gold nanoparticles (GNP, ~200 nm) could induce the heart injury because of the nanoparticle interference

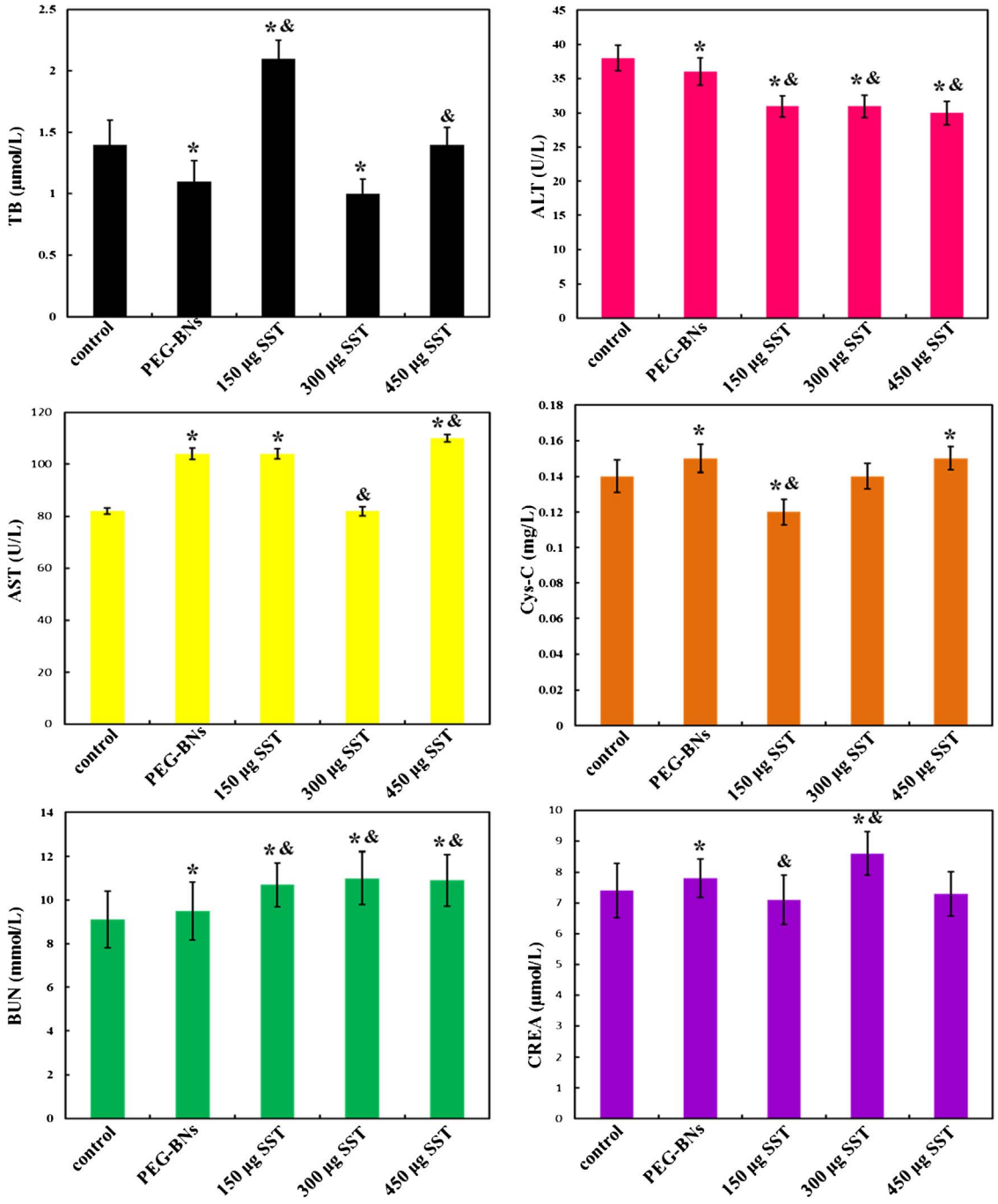

Fig. 8. Biochemical indexes content in serum in SST synergetic group mice (*$p < 0.05$ for the different concentration group *vs.* control group; &$p < 0.05$ for the prevention group *vs.* single PEG-BNs group. ± sem).

with antioxidant defense mechanism. In addition, they also reported that pathological changes would be more obvious for the smaller sizes of nanoparticles, causing significantly sever oxidative stresses. In this work, the size of PEG-BNs was about 20 nm, and therefore, these nanoparticles could lead to a stronger lesion in the heart. Smaller size and high compatibility of PEG-BNs could also enter into kidney during the blood circulation, and then they are excreted out of the body through urine. During this process, the PEG-BNs could cause serve toxicity in the tissues of mice *in vivo*.

In addition, the effect of SST on the toxicity of PEG-BNs to mice was further studied in this work. Compared to the control and single PEG-BNs group mice, from the histology sections results of prevention group and synergistic group mice, it could be seen that the myocardial gap was widened with a slight hemorrhage in heart, and some black nanoparticles also could be seen in the section. The possible reason for the widened myocardial gap could be the rejection of SST to mice, because one of the functions of SST delayed the development of coronary altherosclerosis, including reduction the formation of new lesions and the whole jam as shown in (Fig. 9). It was observed that more black nanoparticles were seen in liver, and hepatic edema and bleeding were produced in liver; the splenic histology was the same with that of the PEG-BN group mice, such as the splenic cell dissolved and bleeding (Fig. 9). In addition, alveolar wall thickening, bronchial epithelial disorder and proliferation of interstitial small blood vessels could also be observed in lung; and the glomerular swelling and edema were also seen in kidney tissue. Interestingly, the serve bleeding was presented in kidney tissue for the synergistic group mice which might be attributed to the improved biocompatibility of PEG-BNs in the

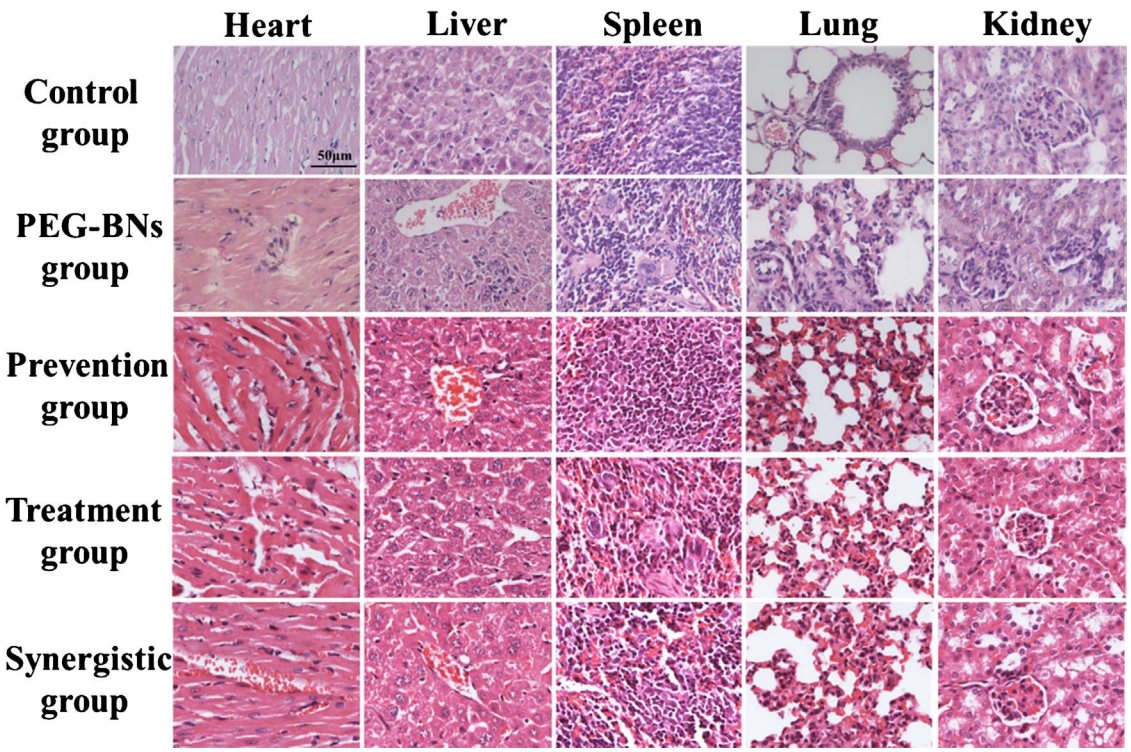

Fig. 9. The histology sections of tissues after exposure PEG-BNs or SST to mice.

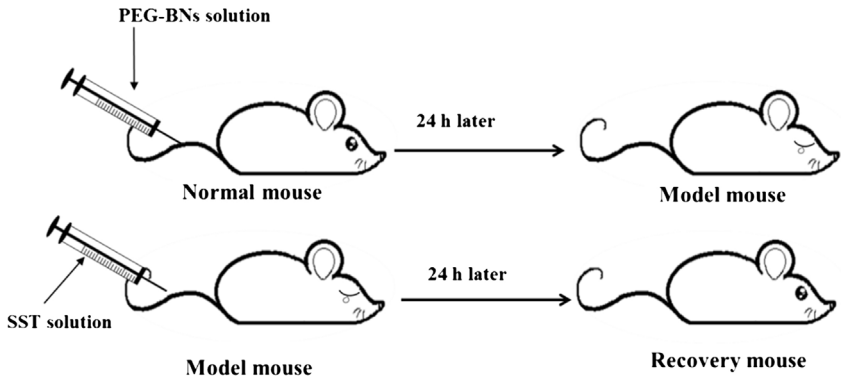

Fig. 10. The illustrative overview about the effect of SST on the toxicity of PEG-BNs in mice.

presence of SST. Therefore, the SST had not prevention or synergistic effects on the toxicity of PEG-BNs to mice *in vivo*.

However, compared with the histology sections of the control group and PEG-BNs group mice, when the SST was injected intravenously into the PEG-BNs model mice, the myocardial gap also was widened for the effect of SST, but the edema and hyperemia were not found except the few black nanoparticles that were seen in heart (Fig. 9). The histology sections of liver and kidney were almost present in the normal state with only few black nanoparticles. But there were more black nanoparticles in spleen than the haemorrhage and edema, which might be resulted in the tissue gap widened caused by the injection of SST. The slight edema and pulmonary congestion could be seen in lung, as well as thickening of alveolus walls which indicate that there were also some damages in these organs. Therefore, the SST has a treatment effect on the damages of PEG-BNs to mice *in vivo* up to certain degree.

In summary, the results of biochemical indexes are consistent with the results of the histology sections. PEG-BNs can serious damage the body health but SST is expected to provide relief to the damage effect (Fig. 10).

4. Conclusion

After exposure PEG-BNs to mice intravenously, they were distributed mainly in liver, spleen, kidney and lung with obvious tissue lesions. Meanwhile, from the results of histology sections and biochemical indexes, the SST showed a significant treatment effect on the damages of PEG-BNs in mice. Therefore, it can be seen that the PEG-BNs still have a serious toxicity to body *in vivo*, but some organic materials such as SST might relief the toxicity of nanoparticles. The interesting results of this work can provide some base data for the toxicity treatment of nanoparticles *in vivo* in the future.

Conflict of interest

The authors declare that their is no conflict of interest.

Acknowledgment

The research project was supported by the National Natural Science Foundation of China No. 31471953.

References

Abaci, O., Ozkan, A.A., Kocas, C., Cetinkal, G., Karaca, O.S., Baydar, O., Kaya, A., Gurmen, T., 2015. Impact of rosuvastatin on contrast-induced acute kidney Iinjury in patients at high risk for nephropathy undergoing elective angiography. Am. J. Cardiol. 115, 867.

Abdelhalim, M.A., Jarrar, B.M., 2011. The appearance of renal cells cytoplasmic degeneration and nuclear destruction might be an indication of GNPs toxicity. Lipids Health Dis. 10, 1–6.

Batista, D., Pascoal, C., Cássio, F., 2017. How do physicochemical properties influence the toxicity of silver nanoparticles on freshwater decomposers of plant litter in streams? Ecotoxicol. Environ. Saf. 140, 148–155.

Carvalho, M.D.F., Melo, L.I.M., Chacon, M.C.M., Farias, D.C.R., Ítalo Medeiros de, A., Rêgo, A.C.M., Medeiros, V.B., Araújo-Filho, I., Medeiros, A.C., 2012. Effect of simvastatin in hepatic ischemia and reperfusion in rats. J. Surg. Clin. Res. 3, 17.

Cheungpasitporn, W., Thongprayoon, C., Kittanamongkolchai, W., Edmonds, P.J., O'Corragain, O.A., Srivali, N., Ungprasert, P., Erickson, S.B., 2015. Periprocedural effects of statins on the incidence of contrast-induced acute kidney injury: a systematic review and meta-analysis of randomized controlled trials. Ren. Fail. 37, 1.

Chhowalla, M., Shin, H.S., Eda, G., Li, L.J., Loh, K.P., Zhang, H., 2013. The chemistry of two-dimensional layered transition metal dichalcogenide nanosheets. Nat. Chem. 5, 263–275.

Ciofani, G., Danti, S., D'Alessandro, D., Moscato, S., Menciassi, A., 2010. Assessing cytotoxicity of boron nitride nanotubes: interference with the MTT assay. Biochem. Biophys. Res. Commun. 394, 405–411.

Ciofani, G., Del, T.S., Rocca, A., De, V.G., Cappello, V., Yamaguchi, M., Li, X., Mazzolai, B., Basta, G., Gemmi, M., 2014. Cytocompatibility evaluation of gum Arabic-coated ultra-pure boron nitride nanotubes on human cells. Nanomedicine 9, 773–788.

Danti, S., Ciofani, G., Pertici, G., Moscato, S., D'Alessandro, D., Ciabatti, E., Chiellini, F., D'Acunto, M., Mattoli, V., Berrettini, S., 2014. Boron nitride nanotube-functionalised myoblast/microfibre constructs: a nanotech-assisted tissue-engineered platform for muscle stimulation. J. Tissue Eng. Regen. Med. 9, 847–851.

De Keyser, C.E., Koehler, E.M., Schouten, J.N., Visser, L.E., Hofman, A., Janssen, H.L., Stricker, B.H., 2014. Statin therapy is associated with a reduced risk of non-alcoholic fatty liver in overweight individuals. Dig. Liver Dis. 46, 720–725.

Elkady, M.F., Strong, V., Dubin, S., Kaner, R.B., 2012. Laser scribing of high-performance and flexible graphene-based electrochemical capacitors. Science 335, 1326–1330.

Endres, M., 2006. Statins: potential new indications in inflammatory conditions. Atheroscler. Suppl. 7, 31.

Ganesh, K., Archana, D., Preeti, K., 2015. Galactosylated albumin nanoparticles of simvastatin. Iran. J. Pharm. Res. 14, 407–415.

Hou, W., Lv, J., Perkovic, V., Yang, L., Zhao, N., Jardine, M.J., Cass, A., Zhang, H., Wang, H., 2013. Effect of statin therapy on cardiovascular and renal outcomes in patients with chronic kidney disease: a systematic review and meta-analysis. Eur. Heart J. 34, 1807.

Joshi, R.K., Carbone, P., Wang, F.C., Kravets, V.G., Su, Y., Grigorieva, I.V., Wu, H.A., Geim, A.K., Nair, R.R., 2014. Precise and ultrafast molecular sieving through graphene oxide membranes. Science 343, 752–754.

Khurana, V., Bejjanki, H.R., Caldito, G., Owens, M.W., 2007. Statins reduce the risk of lung cancer in humans: a large case-control study of US veterans. Chest 131, 1282–1288.

Kochuparambil, S.T., Al-Husein, B., Goc, A., Terris, M., Somanath, P.R., 2011. 410 anti-cancer efficacy of simvastain on prostate cancer cells and tumor xenogafts is mediated through inhibition of KAT. J. Urol. 185 e165–e165.

Li, Z., Geng, Y., Zhang, X., Qi, W., Fan, Q., Li, Y., Jiao, Z., Wang, J., Tang, Y., Duan, X., 2011. Biodistribution of co-exposure to multi-walled carbon nanotubes and graphene oxide nanoplatelets radiotracers. J. Nanopart. Res. 13, 2939–2947.

Lin, L., Li, Z., Zheng, Y., Wei, K., 2009. Synthesis and application in the CO oxidation conversion reaction of hexagonal boron nitride with high surface area. J. Am. Ceram. Soc. 92, 1347–1349.

Liu, B., Wei, Q., Tian, L., Zhan, L., Miao, G., An, W., Dan, L., Jing, L., Zhang, X., Wu, W., 2015. In vivo biodistribution and toxicity of highly soluble PEG-coated boron nitride in mice. Nanoscale Res. Lett. 10, 1–7.

Mosleh, M., Atnafu, N.D., Belk, J.H., Nobles, O.M., 2009. Modification of sheet metal forming fluids with dispersed nanoparticles for improved lubrication. Wear 267, 1220–1225.

Qi, W., Bi, J., Zhang, X., Wang, J., Wang, J., Liu, P., Li, Z., Wu, W., 2014. Damaging effects of multi-walled carbon nanotubes on pregnant mice with different pregnancy times. Sci. Rep. 4, 4352.

Raccichini, R., Varzi, A., Passerini, S., Scrosati, B., 2015. The role of graphene for electrochemical energy storage. Nat. Mater. 14, 271–279.

Raju, K.K., 2014. Factorial design studies and biopharmaceutical evaluation of simvastatin loaded solid lipid nanoparticles for improving the oral bioavailability. ISRN Nanotechnol. 2014, 1–8.

Rezende, N.C.C., Guerra, S.C.P., Fernandes, T.U.G., Macedo, R., Ítalo Medeiros, A., Medeiros, A.C., 2015. Simvastatin effects on skeletal muscle using the biodistribution of 99mTc sestamibi. J. Surg. Clin. Res. 5, 92.

Seiffert, J., Hussain, F., Wiegman, C., Li, F., Bey, L., Baker, W., Porter, A., Ryan, M.P., Chang, Y., Gow, A., 2015. Pulmonary toxicity ofinstilled silver nanoparticles: influence of size, coating and rat strain. PLoS One 10, e0119726.

Sendra, M., Yeste, P.M., Moreno-Garrido, I., Gatica, J.M., Blasco, J., 2017. CeO2 NPs, toxic or protective to phytoplankton? Charge of nanoparticles and cell wall as factors which cause changes in cell complexity. Sci. Total Environ. 590–591, 304–315.

Shah, M., Chuttani, K., Mishra, A.K., Pathak, K., 2011. Oral solid compritol 888 ATO nanosuspension of simvastatin: optimization and biodistribution studies. Drug Dev. Ind. Pharm. 37, 526–537.

Simon, T.G., King, L.Y., Zheng, H., Chung, R.T., 2014. Statin use is associated with a reduced risk of fibrosis progression in chronic hepatitis C. J. Hepatol. 62, 18–23.

Tu, Y., Lv, M., Xiu, P., Huynh, T., Zhang, M., Castelli, M., Liu, Z., Huang, Q., Fan, C., Fang, H., 2013. Destructive extraction of phospholipids from Escherichia coli membranes by graphene nanosheets. Nat. Nanotechnol. 8, 594–601.

Wang, H., Wang, J., Deng, X., Sun, H., Shi, Z., Gu, Z., Liu, Y., Zhao, Y., 2004. Biodistribution of carbon single-wall carbon nanotubes in mice. J. Nanosci. Nanotechnol. 4, 1019–1024.

Wang, Q.H., Kalantarzadeh, K., Kis, A., Coleman, J.N., Strano, M.S., 2012. Electronics and optoelectronics of two-dimensional transition metal dichalcogenides. Nat. Nanotechnol. 7, 699.

Wang, J., Li, C., Tao, H., Cheng, Y., Han, L., Li, X., Hu, Y., 2013. Statin use and risk of lung cancer: a meta-analysis of observational studies and randomized controlled trials. PLoS One 8, e77950.

Weber, A., Bringmann, U., Nikulski, R., Klages, C.P., 1993. Electron cyclotron resonance plasma deposition of cubic boron nitride using N-trimethylborazine. Surf. Coat. Technol. 60, 201–206.

Wei, Q., Zhan, L., Bi, J., Jing, W., Wang, J., Sun, T., Guo, Y.A., Wu, W., 2012. Biodistribution of co-exposure to multi-walled carbon nanotubes and nanodiamonds in mice. Nanoscale Res. Lett. 7, 1–9.

Weng, Q., Wang, B., Wang, X., Hanagata, N., Li, X., Liu, D., Wang, X., Jiang, X., Bando, Y., Golberg, D., 2014. Highly water-soluble, porous, and biocompatible boron nitrides for anticancer drug delivery. ACS Nano 8, 6123–6130.

Wu, C.S., Lin, Z.A., Pan, J.W., Rei, M.H., 2001. A novel boron nitride supported Pt catalyst for VOC incineration. Appl. Catal. A: Gen. 219, 117–124.

Xu, M., Liang, T., Shi, M., Chen, H., 2013. Graphene-like two-dimensional materials. Chem. Rev. 113, 3766–3798.

Yang, K., Wan, J., Zhang, S., Zhang, Y., Lee, S.T., Liu, Z., 2011. In vivo pharmacokinetics, long-term biodistribution, and toxicology of PEGylated graphene in mice. ACS Nano 5, 516–522.

Yang, T.Y., Lin, W.M., Lin, C.L., Sung, F.C., Kao, C.H., 2015. Correlation between use of simvastatin and lovastatin and female lung cancer risk: a nationwide case-control study. Int. J. Clin. Pract. 69, 571–576.

Zhang, H., Chen, S., Zhi, C., Yamazaki, T., Hanagata, N., 2013. Chitosan-coated boron nitride nanospheres enhance delivery of CpG oligodeoxynucleotides and induction of cytokines. Int. J. Nanomed. 8, 1783–1793.